

# The melt anomaly of 2002 on the Greenland Ice Sheet from active and passive microwave satellite observations

K. Steffen,<sup>1</sup> S. V. Nghiem,<sup>2</sup> R. Huff,<sup>1</sup> and G. Neumann<sup>2</sup>

Received 5 May 2004; revised 10 August 2004; accepted 20 September 2004; published 21 October 2004.

[1] Active and passive microwave satellite data are used to map snowmelt extent and duration on the Greenland ice sheet. The passive microwave (PM) data reveal the extreme melt extent of 690,000 km<sup>2</sup> in 2002 as compared with an average extent of 455,000 km<sup>2</sup> from 1979–2003. A statistical analysis of the melt time series affirms an increased melt extent earlier in the melt season. The QuikSCAT (QSCAT or AM) analysis for 1999 to 2004 confirms the extreme melt situation in 2002. QSCAT data show a significant increase in melt season length over several areas in 2003. SSM/I and QSCAT melt data reveal that the later detects melt earlier and is more sensitive to surface melt. QSCAT detects an earlier stage of melt and SSM/I detects a later stage of melt. The SSM/I XGPR melt extent is approximately confined to the QSCAT melt areas experiencing 2 weeks or more of melting time. *INDEX TERMS*: 1827 Hydrology: Glaciology (1863); 1694 Global Change: Instruments and techniques; 3349 Meteorology and Atmospheric Dynamics: Polar meteorology; 3360 Meteorology and Atmospheric Dynamics: Remote sensing. **Citation**: Steffen, K., S. V. Nghiem, R. Huff, and G. Neumann (2004), The melt anomaly of 2002 on the Greenland Ice Sheet from active and passive microwave satellite observations, *Geophys. Res. Lett.*, 31, L20402, doi:10.1029/2004GL020444.

## 1. Introduction

[2] The Greenland ice sheet plays a crucial role in global climate because of its high elevation as a topographic barrier for synoptic scale circulation, and its substantial volume of fresh water stored in the ice mass. Monitoring the Greenland ice sheet melt characteristics is critical to the assessment of ice sheet mass balance and the interpretation of the mass balance observations. Moreover, surface melt can act to enhance the flow of outlet glaciers through crevasse overdeepening and to contribute to the very rapid thinning of a number of outlet glaciers in Eastern Greenland [Zwally *et al.*, 2002]. In this study, we present the melt anomalies of 2002 and 2003 observed with satellite data over the Greenland ice sheet.

## 2. Method

### 2.1. Melt Detection From Passive Microwave

[3] Several PM-based melt assessment algorithms [Mote and Anderson, 1995; Abdalati and Steffen, 1995] are appli-

cable to Scanning Multi-channel, Microwave Radiometer (SMMR) and Special Sensor Microwave/Imager (SSM/I) instruments providing near-continuous coverage since 1979. The PM data as gridded brightness temperatures on polar stereographic grids (25 km resolution) used in this study are from the National Snow and Ice Data Center [Maslanik and Stroeve, 2003], containing daily data spanning 25 melt seasons from 1979 to 2003. Observations from April through October are analyzed (214 days per year). Only pixels without contamination from land are considered ( $1.55 \times 10^6$  km<sup>2</sup> or 2,476 pixels). Melt is detected with the cross polarized gradient ratio (XPGR) [Abdalati and Steffen, 1995, 2001].

[4] Given 25 years of observations for each pixel on each day for the SSM/I data, and for alternating days for the SMMR data of the melt season, we compute the probability that any pixel will melt on any day. We characterize melt on the Greenland ice sheet as a binomial system. Assuming the melt observations are independent, the probability that a pixel will melt  $n$  times during one year with  $N$  possible melt days is given by  $p_N(n) = N!p^nq^{(N-n)}/n!(N-n)!$  where  $p$  is the average number of times the pixel melted per year between 1979 and 2003 and  $q = 1 - p$ .

[5] Similarly, the probability of any pixel melting at least as many times as observed can be computed directly from the binomial distribution. This establishes how anomalous the observed melt was on a pixel-by-pixel basis for each day of a melt season. The likelihood of the entire ice sheet melting as observed for one melt season relative to the 25 years of observations is the product over all pixels of  $(P_{i,j}/P_{random})$ , where  $P_{i,j}$  is the probability of pixel  $i, j$  melting as many times as observed and  $P_{random} = (\text{the sum of the observed melt over all pixels})/(\text{all days} \times \text{all pixels} \times \text{all years})$ . To avoid computational problems associated with very small numbers as a result of multiplying probabilities the log likelihood of each melt season in the dataset is computed.

### 2.2. Melt Detection From QuikSCAT

[6] QSCAT satellite data have been acquired for about half a decade so far by the SeaWinds scatterometer since July 1999. It has an outer swath of 1800 km for vertical polarization and an inner swath of 1400 km for horizontal polarization with a footprint of 25 km. These large swaths cover Greenland 2 times/day around 6:20 am and pm [Nghiem *et al.*, 2001].

[7] To detect and map melt regions on the Greenland ice sheet, we use the diurnal backscatter response to surface melt [Nghiem *et al.*, 2001]. QSCAT data are gridded in 0.25° grid in latitude and longitude and we use the average of all measurements in the pixel separately for ascending and descending passes. We co-located the data from the early morning ( $t_a$ ) in an ascending orbit pass and late

<sup>1</sup>Cooperative Institute for Research in Environmental Sciences, University of Colorado, Boulder, Colorado, USA.

<sup>2</sup>Jet Propulsion Laboratory, California Institute of Technology, Pasadena, California, USA.

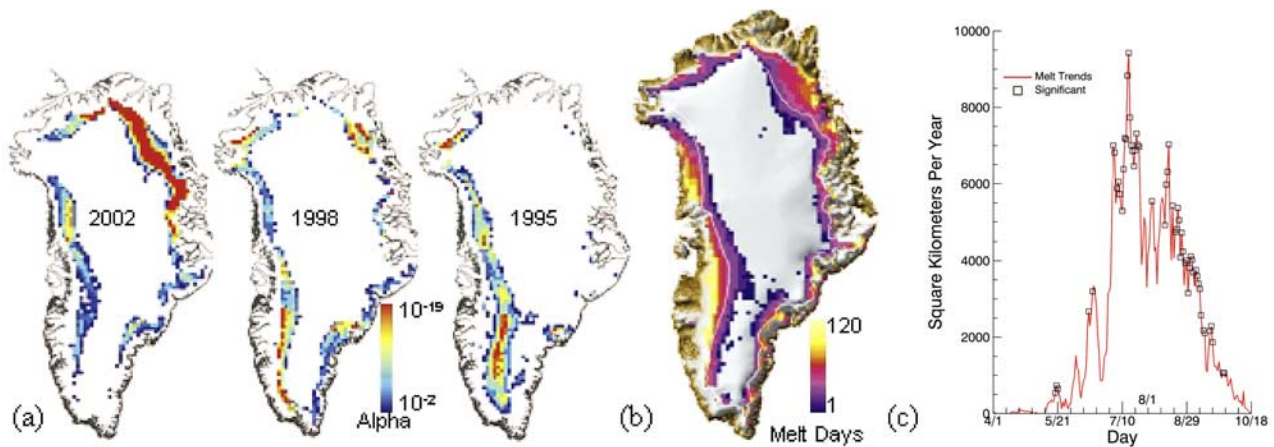


**Figure 1.** (a) The probability of a pixel melting at least as many times as observed during the 1995, 1998 and 2002 melt seasons given the last 25 years of melt observations. (b) Melt extent for 2002: Pixels are color coded for number of melt days during the season. (c) Slopes of the trend lines fit to the areas observed to melt between April and November from 1979 to 2003. Days with a trend that is significantly different from zero (alpha of 0.1 and N of 25) are highlighted by a red square. Peak melt expectation is near the first of August.

afternoon ( $t_p$ ) in a descending pass for each day. The diurnal backscatter change is defined as the backscatter difference in the decibel (dB) domain as  $\Delta\sigma_{VV} = \sigma_{VV}(t_p) - \sigma_{VV}(t_a)$  [Nghiem *et al.*, 2001], where  $\sigma_{VV}$  is the vertical-polarization backscatter and all quantities are in dB. The criteria for the melt detection is based on  $|\Delta\sigma_{VV}|$  greater than 1.8 dB for melt and less than 1.0 dB for refreeze, based on relative backscatter change within 12 hours (between morning and evening data), which allows the use of the simple threshold method without relying on absolute backscatter value [Nghiem *et al.*, 2001].

[8] For each melt season, we can determine the first and the last melt dates. Between these dates, the ice can melt and refreeze on different days. Using the melt detection results for each melt season, we can count the number of melting days and map the results over the entire Greenland ice sheet.

### 3. Results

#### 3.1. Statistical Analysis for Passive Microwave Derived Melt

[9] Suppose a pixel in northeastern Greenland is observed to melt 42 times during the melt season of 2002. How anomalous is this observation? Knowing that the pixel has been observed to melt on average 17 times per year from 1979 through 2003 and assuming a binomial system, we compute the probability of the pixel melting at least 42 times ( $5.9 \times 10^{-12}$ ). Figure 1a shows the probabilities of the observed melt behavior on the Greenland ice sheet for several large melt years and indicates the extreme melt anomaly observed in northeastern Greenland in 2002.

[10] Prior to 2002, both 1995 and 1998 were extreme melt years in terms of maximum areal extent and total melt. During 1995 melt was dominated by a high frequency of melt along the western margin of the ice sheet. During 1998 melt was spatially diverse with slightly more melt than usual in the northeast and southwest. However, the high frequency melt in 2002 in the northeast and along the western margin is unprecedented in the PM record with a

log likelihood of occurrence that is 35% lower than the previous record melt anomaly in 1991.

[11] The average melt area as a function of day of the year is normally distributed with peak melt expected on or about August 1. However, the variance is skewed toward earlier in the melt season with peak variance observed around July 15. This indicates that the amount of melt that can be expected prior to August has changed over the last 25 years as a result of increased melt extents earlier in the melt season. The amount of melt occurring on July 15 has increased by over 9,000 km<sup>2</sup> per year since 1979. This trend is significant at the 0.01 level. Figure 1c depicts the magnitude of the increasing trends in melt extent on a daily basis over the last 25 years. Although there is a large amount of inter-annual variability in melt extent on a given day, 56 days show statistically significant (alpha = 0.1) increasing trends in melt area.

[12] The melt extent, defined as the area of the ice sheet that melted at least once during the melt season was nearly 690,000 km<sup>2</sup> in 2002 as compared with an average melt extent of 455,000 km<sup>2</sup> from 1979–2003. The largest extent prior to 2002 was 627,500 km<sup>2</sup> in 1995 when the entire ice sheet south of 67° N melted. Melt along the west coast was extensive during 2002 but not atypical for large melt years. However melt in the north and northeast was highly irregular both in terms of extent and frequency. Nearly 3,000 km<sup>2</sup> (Figure 1b) were classified as melting during 2002 that had not previously melted during any other year between 1979 and 2003.

#### 3.2. Recent Melt Observed by QuikSCAT

[13] First, we show results around the ETH/CU AWS (69°34′03″N and 49°19′17″W) to compare QSCAT melt observations and Greenland Climate Network (GC-Net) measurements. We extract 5 year (1999 to 2004) of QSCAT data within a radius of 25 km around this AWS. Figure 2 presents QSCAT backscatter and diurnal signatures, and ETH/CU AWS air temperature.

[14] QSCAT measurements around ETH/CU Camp can determine the melt timing in terms of the first and last melt

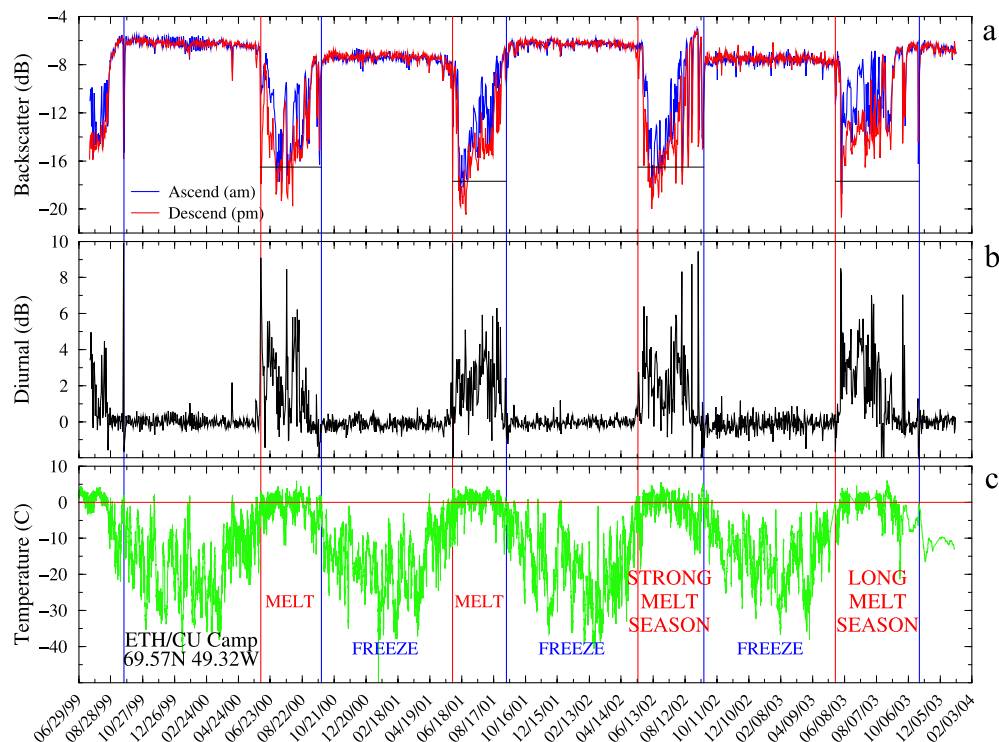


**Figure 2.** Half-decade records for ETH/CU Camp station: (a) Top panel for QSCAT backscatter, (b) middle panel for QSCAT diurnal signature, and (c) bottom panel for air temperature measured at the AWS site. First melt dates are marked with vertical red lines, and last melt dates with vertical blue lines. Horizontal bars in the top panel mark backscatter level at 10 dB lower than that before the first melt.

dates as marked by the vertical lines in Figure 2. We use the backscatter level change of 10 dB or one order of magnitude for our melt threshold. Such a large backscatter drop corresponds to microwave attenuation caused by increased wetness due to strong melt. QSCAT results indicate that: (a) first melt date was on 5 June 2000, 1 June 2001, 16 May 2002, and 22 May 2003; (b) last melt date was on 22 September 1999, 27 September 2000, 10 September 2001, 17 September 2002, and 27 October 2003; and (c) melt season lengths were 114, 101, 124, and 158 days for years 2000–2003 respectively, with the strongest melt occurring in 2002 (Figure 2). The melt timing and melt season lengths have large interannual variabilities with a lengthening of melt season in 2002 and a longer melt period in 2003. Air temperature data from the ETH/CU Camp AWS support the QSCAT melt results.

[15] The melt timing and melt season length for ETH/CU Camp reveal that 2002 has the earliest melt and the second longest melt season length in 1999–2004. Assuming the same melt season length, early melt timing is more important because it is closer to the summer solstice (stronger insolation flux) compared to late freeze-up. Thus, the 2002 early melt could cause the strong melt in that year. For 2003, the first melt date was later than that in 2002 but still rather early compared to 2000 and 2001. This example illustrates the complex changes in summer melt, and melt strength alone is not sufficient to characterize an overall melt season that also depends on melt timing and melt length.

[16] We now use QSCAT data to observe melt not only at a given area such as ETH/CU Camp, but also over all regions of the Greenland ice sheet on the daily basis.

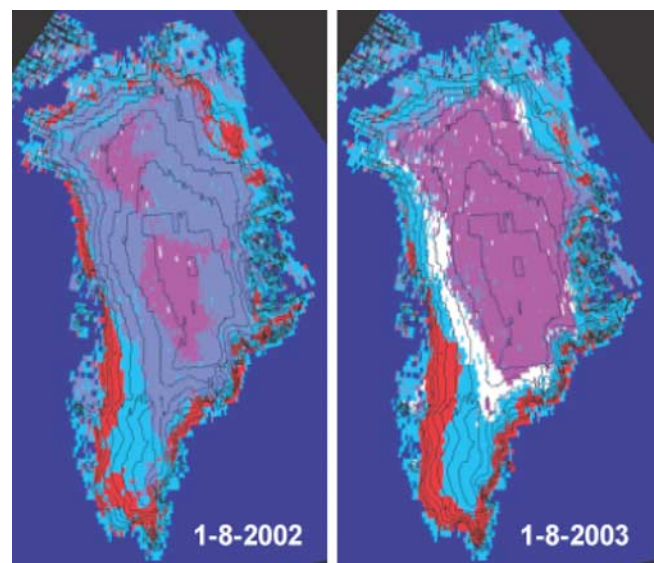


**Figure 3.** QSCAT melt maps on the climatological peak-melt day (1 August). Red color represents current active melt areas, light blue is for areas that have melted but currently refreeze, white is for areas that will melt later, and magenta is for areas that do not experience any melt throughout the melt season. The dark blue color surrounding Greenland is the ocean mask.

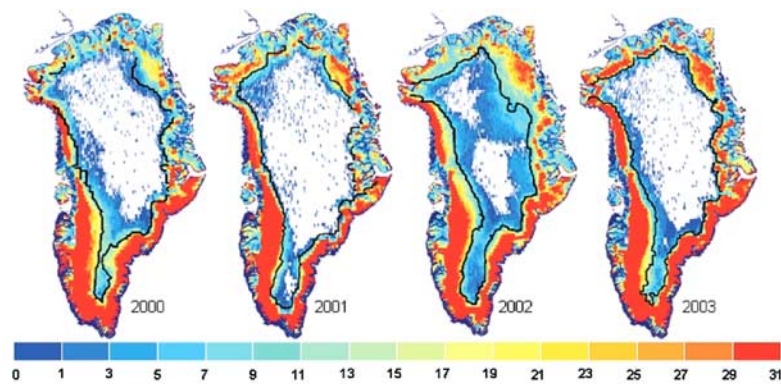


**Figure 4.** QSCAT maps of number of melt days (violet to red for 1 to 31 days) in 2000–2003 with the overlaid black contours representing melt extent derived from PM data.

Figure 3 shows melt maps derived for the climatological peak-melt day (1 August) for years 2002–2003. Contours of Greenland topography on QSCAT maps are overlaid in Figure 3 to observe the relationship between melt and the landscape.

[17] QSCAT mapping can reveal details of the spatial pattern of surface melt evolution in time. There are large variabilities in melt extent and melt timing over different regions. Figure 3 confirms that 2002 has the most extensive areal melt. In 2002, the northeast quadrant of the Greenland ice sheet, extending well into the dry snow zone, experienced at least some melt where melt never happened before (from satellite data records to date). Since the beginning of the QSCAT data record (July 1999), the smallest spatial extent of melt occurred in 2001, and melt extent was similar for years 2000 and 2003.

[18] On the climatological peak melt day, there was almost no white area left over in 2002 as seen in Figure 3. This indicates that melt and/or refreeze had already occurred some time before the peak melt over the total melt extent for 2002. In contrast, year 2003 had significant white areas remaining at the peak melt, which would not be melted until a later time. The combination of early melt and late freeze-up makes the 2003 melt season length the longest over many areas as supported by measurements at various AWS sites.

### 3.3. Comparison of PM and QuikSCAT Results

[19] In general, we observe that QSCAT detects melt earlier than the XPGR PM method, and that QSCAT melt areas are larger than PM melt areas. It is worth mentioning that PM single channel algorithm (37 GHz) show melt occurring 5–7 days earlier than the XPGR method [Anderson *et al.*, 1996]. Active backscatter is sensitive to the imaginary part ( $Im\{\epsilon_{eff}\}$ ) of the effective dielectric constant of snow while passive brightness temperature is dependent on the magnitude  $|\epsilon_{eff}|$  of the dielectric constant [Ulaby *et al.*, 1982]. A small amount of wetness in snow can significantly change  $Im\{\epsilon_{eff}\}$  while more wetness is necessary to change  $|\epsilon_{eff}|$ . Therefore, the scatterometer can start to detect an earlier or weaker stage of melt and the XPGR PM method can detect a later or stronger stage of melt. However, QSCAT and PM data are obtained at different frequencies and the above relationship needs to be verified.

[20] To provide a direct comparison of PM and QSCAT results, we overlay results for PM melt extent and QSCAT number of melt days in Figure 4 for years 2000–2003. PM XPGR melt extent is approximately confined to QSCAT melt areas experiencing 2 weeks or more of melting time (Figure 4). QSCAT melt areas outside of the PM melt extent represent the surface that has less melt corresponding to about 15 melt days or less. This is consistent with the relationship of relative melt strength measured by active and passive data as discussed above. Note that such areas can total up to a large region in year 2002. Surface albedo can reduce considerably once the snow melts for a period of 2 weeks. The albedo reduction may significantly impact the surface heat balance and thus change the mass balance. The large number of melt days around the northern perimeter of the ice sheet, which is shown as the narrow dark-red band in north Greenland in the 2003 map was an anomalous feature (Figure 4). This band was wider as defined by the PM melt extent in 2002 than in 2003. However, there were more QSCAT melt days in the 2003 northern melt band.

[21] The comparison reveals that the PM cross-polarized gradient algorithm classifies melt more conservatively than the scatterometer algorithm. The active microwave identifies melt approximately up to two weeks more than the PM at higher elevation in the percolation zone toward the dry snow zone (Figure 4). Both methods (active and passive microwave) consistently identify melt areas that have a melt duration of at least 10–14 days. The longer snowmelt duration can be sufficient to decrease surface albedo and affect surface heat and mass balance.

[22] **Acknowledgments.** The research carried out at JPL, California Institute of Technology, was supported by the National Aeronautics and Space Administration (NASA). The research by CIRES, University of Colorado, was supported by NASA's Cryospheric Sciences.

### References

- Abdalati, W., and K. Steffen (1995), Passive microwave-derived snow melt regions on the Greenland ice sheet, *Geophys. Res. Lett.*, *22*, 787–790.
- Abdalati, W., and K. Steffen (2001), Greenland ice sheet melt extent: 1979–1999, *J. Geophys. Res.*, *106*, 33,983–33,989.
- Anderson, M. R., T. Mote, and W. Abdalati (1996), A comparison of passive microwave techniques for detecting snowpack melt on the Greenland ice sheet, *Rep. on Glacier, Ice Sheets and Volcanoes 96-27*, Cold Regions Res. and Eng. Lab., Hanover, N. H.

- Maslanik, J., and J. Stroeve (2003), *DMSP SSM/I Daily Polar Gridded Brightness Temperatures* [CD-ROM], <http://nsidc.org/data/nsidc-0001.html>, Natl. Snow and Ice Data Cent., Boulder, Colo.
- Mote, T. L., and M. R. Anderson (1995), Variations in snowpack melt on the Greenland ice sheet based on passive-microwave measurements, *J. Glaciol.*, *41*, 51–60.
- Nghiem, S. V., K. Steffen, R. Kwok, and W. Y. Tsai (2001), Detection of snowmelt regions on the Greenland ice sheet using diurnal backscatter change, *J. Glaciol.*, *47*, 539–547.
- Ulaby, F. T., R. K. Moore, and A. K. Fung (1982), *Microwave Remote Sensing*, vol. 2, *Radar Remote Sensing and Surface Scattering and Emission Theory*, Artech House, Norwood, Mass.
- Zwally, H. J., W. Abdalati, and T. Herring et al. (2002), Surface melt-induced acceleration of Greenland ice-sheet flow, *Science*, *297*, 218–222.

---

R. Huff and K. Steffen, Cooperative Institute for Research in Environmental Sciences, University of Colorado, Boulder, CO 80309-0216, USA. (koni@seaice.colorado.edu)

G. Neumann and S. V. Nghiem, Jet Propulsion Laboratory, California Institute of Technology, Pasadena, CA 91109, USA.